Kufa Journal of Engineering
Vol. 16, No. 4, October 2025, P.P. 658-679
Article history: Received 10 March 2025, last revised 1 May 2025, accepted 1 May 2025

EXPERIMENTAL INVESTIGATION OF THE PERFORMANCE OF FIBROUS REINFORCED CONCRETE DEEP BEAM WITH VARIOUS SIZE OF SQUARE WEB-OPENING

Dhyaa A. Al-Sattar[1] and Jasim A.Abdulla[2]

[1] Department of Civil Engineering, University of Mosul, Mosul, Iraq, Email dhyaa.23enp47@student.uomosul.edu.iq

[2] Department of Civil Engineering, University of Mosul, Mosul, Iraq, Email jassim24676@uomosul.edu.iq

https://doi.org/10.30572/2018/KJE/160439

ABSTRACT

This study aims to experimentally investigate the performance of steel fiber-reinforced concrete deep beams with various sizes of square web-opening applied to shear and shear-bending control loading scenarios. Twelve specimens were distributed to two groups according to loading control (shear & shear-bending). Each group consist of three beams prepared of fibrous concrete and others prepared of normal concrete. The three specimens consists of one that is solid as a reference and others containing various-sized square web openings (200 mm & 300 mm). The test results show that all the tested beams failed as shear failure except for the solid beams under shear-bending control, which failed as flexural failure. The presence of square openings with sharp corners and edges leads to high stress concentration, especially when these openings are located in the natural load transmission path. Steel fibers maintain the linear behavior in deep beams with openings until late loading stages, as evident in load-deflection curves. Fibrous beams with openings remained nearly identical. Unlike normal concrete beams, there was a large difference in the load-deflection curves since the early stages of loading. The tested beams failed after yielding of steel reinforcement, as the steel strain of fibrous specimens was lower than that of normal concrete. Steel fibers contributed to reducing stresses in reinforcing steel. Fibrous beams exhibit higher stiffness than normal beams, largely due to the presence of steel fibers. These fibers provide additional tensile strength, resisting shear cracks. Additionally, fibers increase the ductility index and absorption energy, redistributing stresses and provide warning before failure.

KEYWORDS

Deep beam, Web-Opening, Steel fiber, Shear control, Shear-bending control.

1. INTRODUCTION

Reinforced concrete Deep beams are structural elements commonly used in high-rise buildings to transfer high axial loads from upper floors and columns to foundations and soil. They also have many applications in bridges, tanks, offshore structures, and foundation walls (Jasim et al., 2019) (Nayak, 2022). Deep beams are "members loaded on one face and supported on the opposite face such that strut-like compression elements can develop between the loads and supports" and have a clear span to total depth ratio is less than four and shear span to an effective depth less than two. Also, concentrated loads are located at a distance of 2h from the support's face (318, ACI Committee-2019). Creating various types and shapes of openings in reinforced concrete deep beams is necessary for the passage of some services such as electrical, mechanical, sewage, computer networks, and air conditioning systems (El-Kareim et al., 2020). These openings often interrupt the natural load path and stress distribution and also lead to a significant decrease in the ultimate load and stiffness of these beams (Ketab and Attyia, 2024) (Saleh et al., 2023). The existence of an opening within the shear span reduces the load-carrying capacity of the deep beam (Hussain, 2018). Therefore, because concrete is weak in tension, researchers have turned to some techniques and solutions to strengthen these deep beams, including fibers of various types, such as glass or carbon fibers, etc. Steel fibers are a very suitable solution, as they are added to the concrete mixture and lead to enhanced hardness and durability and improved mechanical properties, in addition to their significant effect on reducing cracks, increasing maximum loads, stiffness, etc. They are also an important factor in reducing traditional crowded reinforcement and implementing curved shapes (Olivera, 2010). Many parameters were tested in reinforced concrete deep beams, such as the location, size, and shape of the openings; the shear span to the overall depth ratio (a/d); The results showed that increasing the steel fiber content leads to an increase in the ultimate load of the deep beams (with or without openings). The ultimate load capacity also increases with a decrease in the shear span to depth ratio (a/d) (Vengatachalapathy et al., 2010) (Al-Sarraf et al., 2011). The failure mode depends mainly on the location of the opening. It was observed that when the opening is placed in the midspan of the beams, the behavior of these beams will be similar and close to the behavior of solid beams (Campione and Minafò, 2012). Placing the opening at the top and bottom of the shear span (outside the natural load path) reduces cracking and increases the maximum load (Shaker et al., 2019). The ultimate strength of the beams was significantly reduced when the openings were located within the compression member (struct), and the location of the openings did not significantly affect the ultimate strength in the case of small openings (AL-Bayati et al., 2016) (Mabrouk et al., 2021). In reinforced concrete continuous deep beams with openings, the location of openings in the external or internal shear span of these beams leads to a significant decrease in the ultimate load. Therefore, it is preferable to locate openings in the midspan region (Khalaf and Al-Ahmed, 2021) (Al-Mahbashi et al., 2023). In multi-story buildings, it is possible for reinforced concrete deep beams in the lower floors to carry high concentrated loads from the columns of the upper floors. The presence of square or circular openings in these beams will result in significant weakening of these beams, making this issue very important. This is especially true when the openings are located in the zone of maximum shear force and zero bending moment (shear control), as shown in Fig. 1. Although there are many studies specialized in studying the behavior and performance of reinforced concrete deep beams, solid and with openings and the conclusions reached by researchers about the importance and role of steel fibers in strengthening and improving concrete deep beams, there is a lack of research specialized in studying the behavior of reinforced concrete deep beams when these openings are located in the zone of maximum shear force and zero bending moment (shear control) and in the zone of maximum shear with low bending moment (shear-bending control)

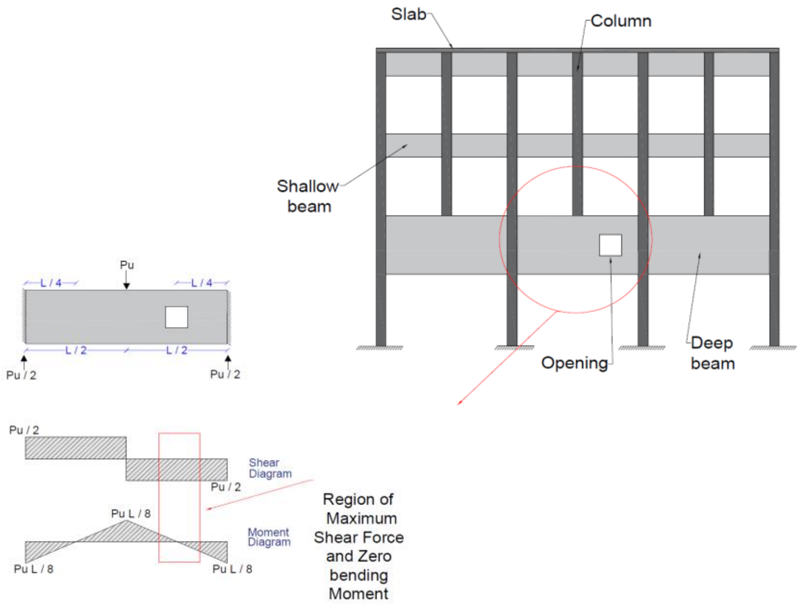

Fig 1. Continuous deep beam with opening located in zone of Maximum shear force and zero bending Moment

This study aims to investigate the effect of adding steel fibers to reinforced concrete deep beams applied to the following two cases:

1. Investigating the performance of fibrous reinforced concrete deep beams containing different sizes of square openings located in the zone of maximum shear and zero bending moment (shear control) Fig. 2-a.

2. Investigating the performance of fibrous reinforced concrete deep beams containing

different sizes of square openings located in a side of span under three-point loading, zone of maximum shear with low bending moment (shear-bending control) Fig. 2-b.

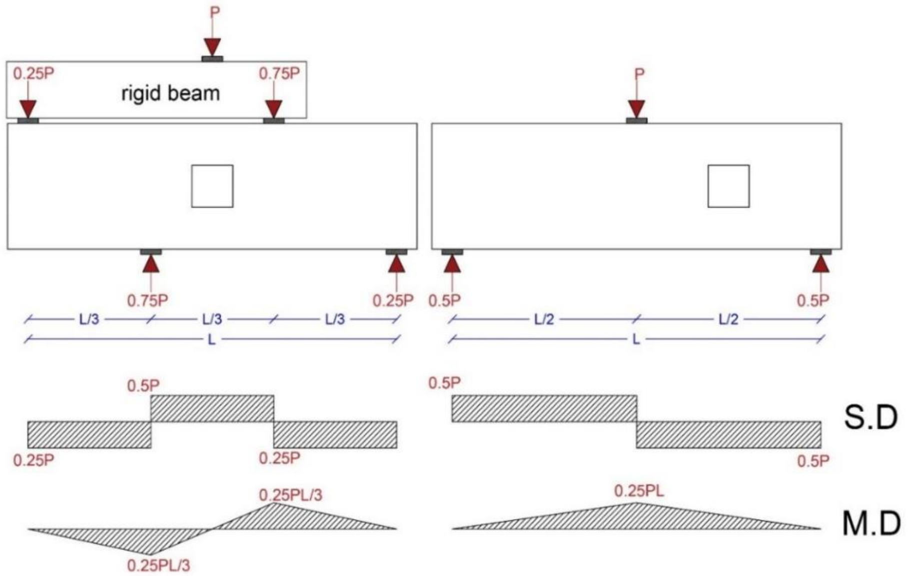

(a) Shear control (b) Shear-bending control

Fig. 2. Applying load and location of opening for shear control and shear-bending control

2. EXPERIMENTAL SPECIMENS DETAILS

In this study, twelve reinforced concrete deep beams with and without square openings were prepared and tested. The specimens were divided into two groups. The first group consisted of six deep beams tested under the shear control case, while the second group included six deep beams tested under the shear-bending control case. In each group, there were three beams of normal concrete, and others contained steel fibers with 0.75% of the concrete mix volume. In each group and for both normal and fibrous reinforced concrete deep beams, there was a solid deep beam as a reference, the second deep beam had a square opening (200 x 200 mm), and the third deep beam had a square opening (300 x 300 mm). Fig. 3. shows parameters of experimental deep beam specimens.

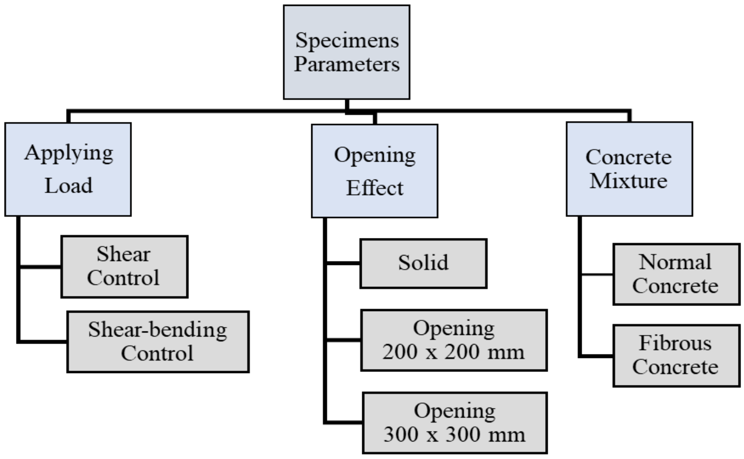

Fig. 3. Parameters of experimental deep beam specimens

The dimensions of each beam were (2000) mm length, (1800) mm clear span, (600) mm depth, and (150) mm width. For easy identification of the beams, the specimens are named as follows, for example: (FC-B-W200), FC indicated the beams as fibrous concrete beams and NC for normal concrete beams, and B indicated Shear-bending control case S for the case of shear control, W200 indicates the size of the square opening is (200 x 200) mm, W300 for opening (300 x 300) mm, and WO for beams without opening. Table 1 shows all details of deep beams used in this study.

All beams were reinforced based on the requirements of the (ACI Code 318-19). Deformed steel bars with diameters of 10 mm and 12 mm were used for reinforcement. The reinforcing steel was tested according to (ASTM A615/A615M-22). The yield stress and ultimate strength for Ø10 mm are 522 MPa and 760 MPa, and for Ø12 mm are 610 MPa and 803 MPa, respectively. 3Ø12 mm rebar is used for bottom longitudinal reinforcement (flexural reinforcement), and 2Ø10 mm is used for top longitudinal reinforcement. The horizontal and vertical shear reinforcement is Ø10@275 mm and Ø10@300 mm, respectively. Vertical shear reinforcement was intensified at a distance of 50 mm at load application points and supports to avoid crushing failure of the concrete during the testing of the specimens. In addition, 2Ø10 mm with (L = 70 cm) is added at the top and bottom openings as additional reinforcement. One strain gauge (S.G.) was placed for each deep beam. (S.G) was placed within the expected load path on the longitudinal steel and the compensation steel around the openings. Fig. 4 and Fig.5. show the reinforcement details and location of the strain gauge for all tested deep beams.

Table 1. Experimental specimens details

Group NO	Beam NO	Concrete mix	Load control	Opening size (mm)	Specimens designation
G_1 (Shear-Bending)	1	Normal	Shear-Bending	------	NC-B-WO
	2	Normal	Shear-Bending	200 x 200	NC-B-W200
	3	Normal	Shear-Bending	300 x 300	NC-B-W300
	4	Fibrous	Shear-Bending	------	FC-B-WO
	5	Fibrous	Shear-Bending	200 x 200	FC-B-W200
	6	Fibrous	Shear-Bending	300 x 300	FC-B-W300
G_2 (Shear)	7	Normal	Shear	------	NC-S-WO
	8	Normal	Shear	200 x 200	NC-S-W200
	9	Normal	Shear	300 x 300	NC-S-W300
	10	Fibrous	Shear	------	FC-S-WO
	11	Fibrous	Shear	200 x 200	FC-S-W200
	12	Fibrous	Shear	300 x 300	FC-S-W300

3. MATERIALS PROPERTIES

Wooden formworks, as shown in Fig. 6, were made of plywood for the purpose of casting the reinforced concrete deep beam specimens. Ordinary Portland cement was used, and the chemical and physical properties were tested according to the Iraqi specification (I.O.S. 5/1984). Fine aggregate and coarse aggregate with a maximum size of 12.5 mm were used, and the aggregates were tested according to the Iraqi specification (I.O.S. 45/1984). The steel fibers were crimped steel fibers with a tensile strength of up to 1100 MPa. Fig. 7 shows the properties of steel fibers used in this study. The concrete mix was designed with a compressive strength of up to 30 MPa, and the mix proportion is (1:2.1:2.76) for cement, gravel, and sand, and the water/cement ratio is (0.48). Table 2 shows the weights of materials used in the casting process. The cube (150 x 150 x 150 mm) was tested according to (BS-1881-116), where the average compressive strength at 28 days was found to be 31 MPa for normal concrete and 33 MPa for fibrous concrete

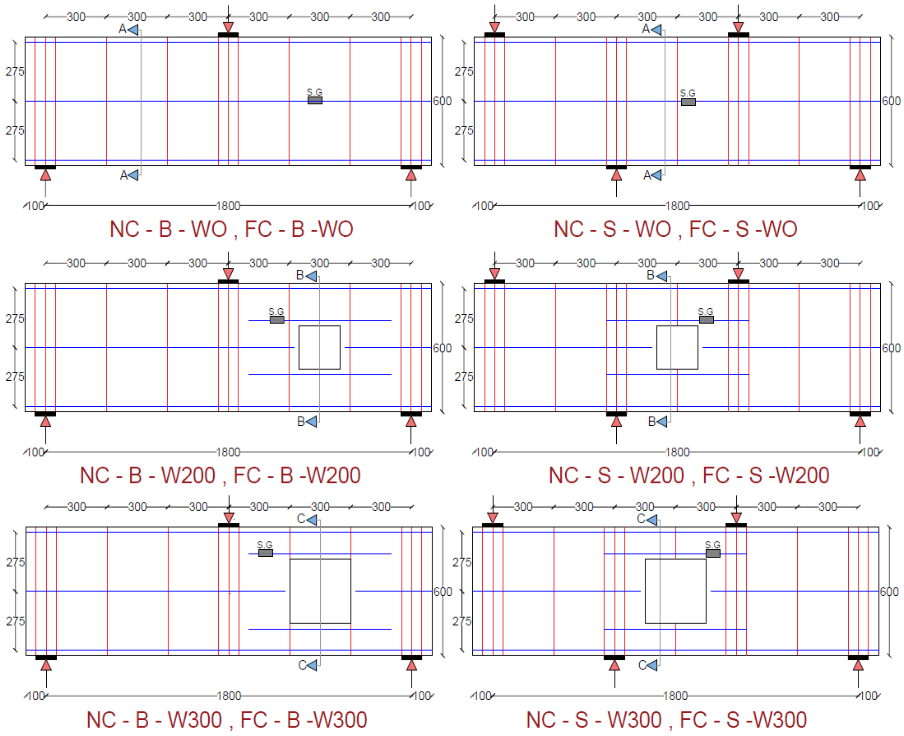

Fig. 4. Reinforcement details of experimental specimens

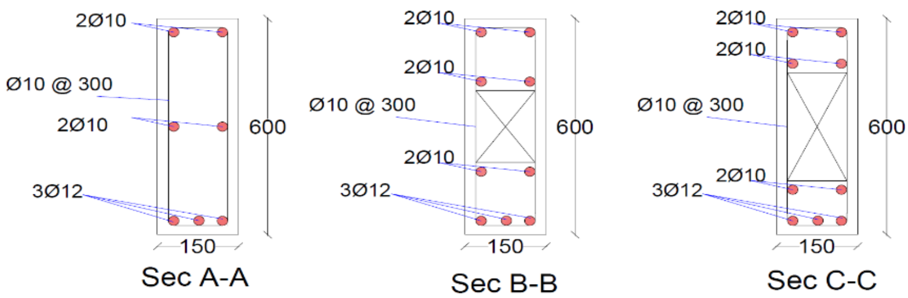

Fig 5. Reinforcement cross section

Fig. 6. Molds and Arrangement of steel reinforcement

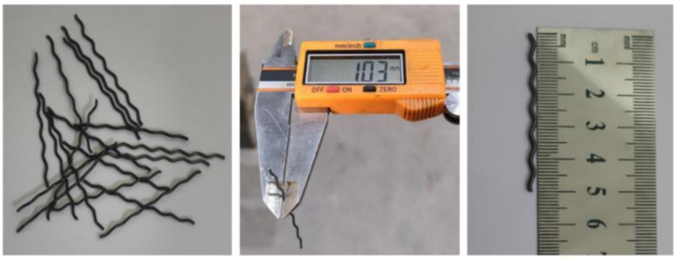

(a) Crimped Steel Fiber (b) Fiber diameter (1.03 mm) (c) Fiber length (5 cm)

Fig. 7. Properties of crimped steel Fiber

Table 2. Mix Proportions For C30 MPa

Material	Cement	Sand	Gravel	water	Steel fiber
Mix Proportions (Kg /m^3)	380	800	1050	185	94

4. CASTING AND TESTING SETUP

A rotary mixer is used to cast twelve reinforced concrete deep beams. six deep beams as normal concrete (NC) and others as fibrous concrete (FC) with 0.75% steel fiber as volume fraction in concrete mix. A vibrator table was used as a compaction process, and the mix was finished and leveled using a surface finishing leveling tool. Fig. 8-a shows the casting of deep beam specimens. The wooden formworks were opened and removed after 24 hours of the casting process, and the casting specimens were covered with burlap bags to maintain moisture for 28 days, as shown in Fig. 8-b. The deep beam specimens were prepared for testing at the Constructional Material Testing Laboratory/Department of Civil Engineering, University of Mosul. To facilitate viewing the cracks and to ensure a good examination, all beams were painted white and coded as shown in Fig. 8-c. The beams were tested using a device with a capacity of 1000 kN. Monotonic load was applied to all specimens. Readings were recorded for each 5 kN increment. All instruments and devices were adjusted and calibrated prior to testing. A linear variable differential transformer (LVDT) was placed at the bottom center of each deep beam for the purpose of recording the deflection for each specified load increment. Fig. 8-d shows the deep beam specimens under the testing setup

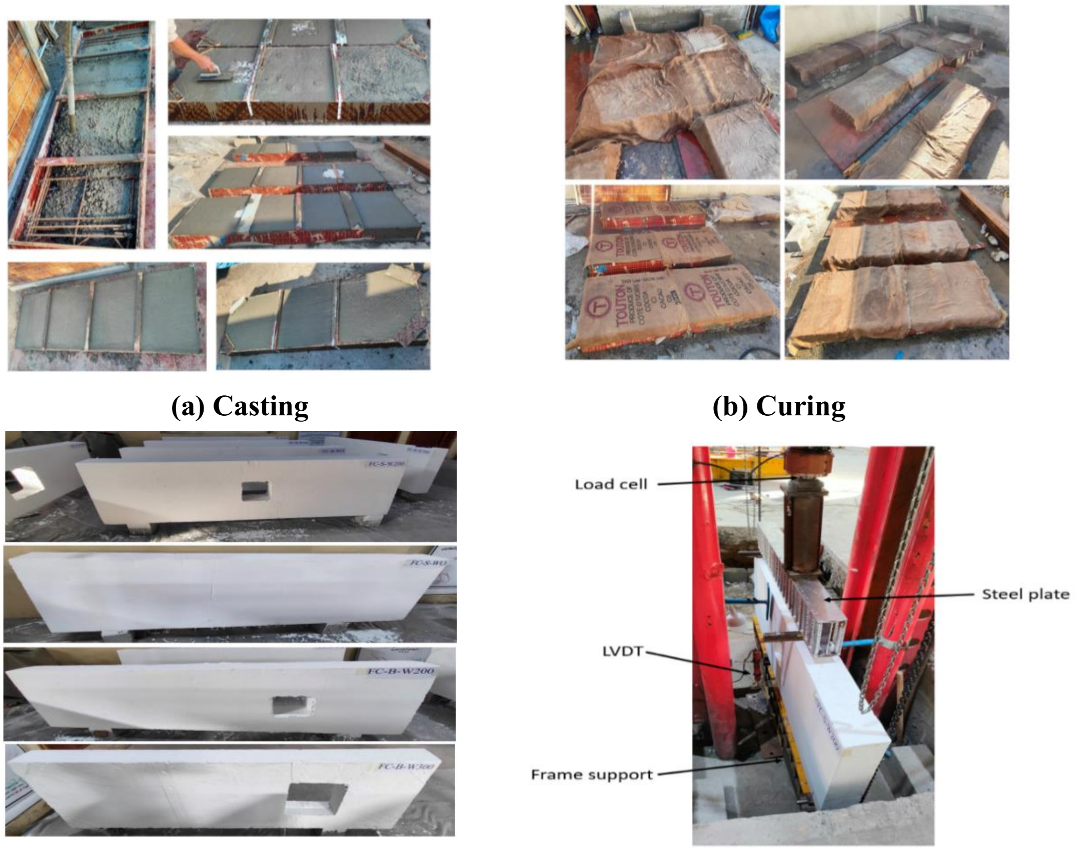

(a) Casting (b) Curing

(c) painting (d) Testing setup

Fig. 8. Casting , curing, panting and testing setup

5. RESULTS AND DISSCUSION

5.1. Crack Pattern and Mode of Failure

Fig. 9 shows the crack pattern of the tested beams at the ultimate load. For the solid beams, the appearance of flexural cracks preceded the appearance of shear cracks. Flexural cracks appeared for the beam (NC-B-WO) at mid-span at 42% of the failure load, while diagonal shear cracks appeared at 48% of the failure load. As for the beam (FC-B-WO), flexural cracks appeared at 36% of the failure load, while a shear crack appeared at 66% of the failure load. This can be attributed to the effect of steel fibers on delaying shear cracks in particular. The above-mentioned beams failed under flexural failure. While the other beam failed as a shear failure. For reinforced concrete beams with square openings. Cracks started to appear at the top and bottom corners of the openings and were mostly diagonal cracks (shear cracks). These cracks continue to expand diagonally along the axis connecting the support and the applied load points. Then, flexural cracks started to appear in the midspan of the deep beams and gradually increased. With increasing loads, the width of shear cracks around the openings started to increase significantly. The final failure of these beams was a shear failure due to the formation of diagonal tensile stresses resulting from the combination of horizontal flexural stresses and diagonal shear stresses. In general, steel fibers played a role in delaying the appearance of initial cracks in the beams, whether shear or flexural cracks. Table 3 shows the first flexural and shear cracking load and the failure mode of the tested beams

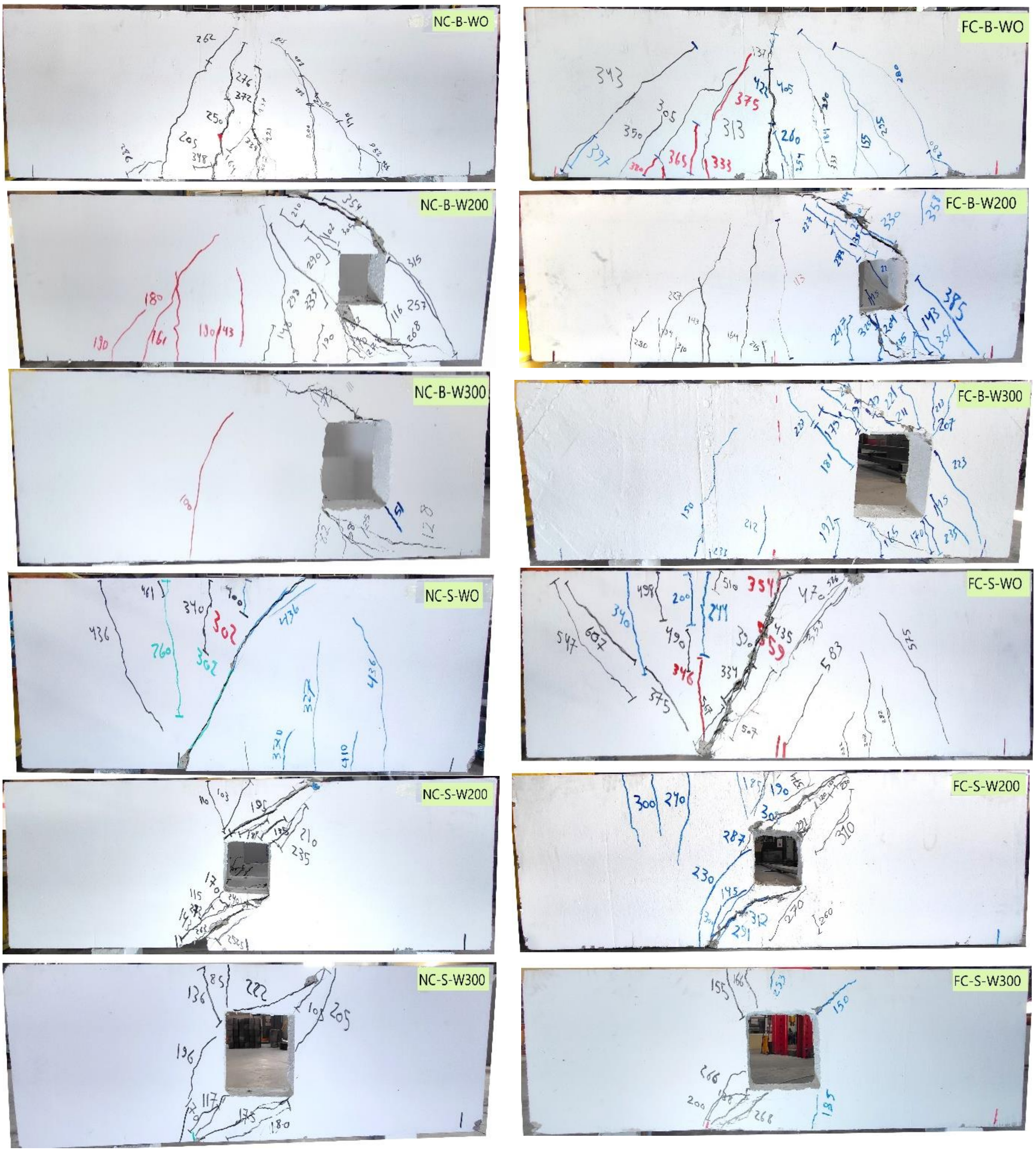

Fig. 9. crack pattern of tested deep beams at ultimate load

5.2. Load -deflection response

The load-deflection curve for all tested deep beams is shown in Fig. 10. Linear behavior can be observed in all tested beams during the initial loading stages, as the deflection curve for all beams is linear. It can be observed that the load-deflection curve for the solid beams NC-B-WO and FC-B-WO, as shown in Fig. 10-a and Fig. 10-b, took on a flat character in the late stages of loading. This confirms that the absorption energy of solid beams is higher than the beams containing square openings, as the failure was sudden when those beams with openings reached the ultimate load. The steel fibers play a major role in maintaining the linear behavior until late stages of loading, and this can be clearly seen in the beams containing openings. The fibrous deep beam with openings (300 mm) was almost identical to the fibrous deep beam with openings (200 mm) until the late stages of loading, in contrast to the beams with normal concrete, where there was a large difference in the curves since the early stages of loading.

Table 3. Cracking load and failure mode

Group No	beam NO	F_{cr}	S_{cr}	Failure Mode
G_1(Shear-Bending)	NC-B-WO	164	190	Flexural
	NC-B-W200	148	102	Shear
	NC-B-W300	82	51	Shear
	FC-B-WO	155	280	Flexural
	FC-B-W200	113	135	Shear
	FC-B-W300	93	212	Shear
G_2 (Shear)	NC-S-WO	180	302	shear
	NC-S-W200	103	135	Shear
	NC-S-W300	85	105	Shear
	FC-S-WO	200	287	Shear
	FC-S-W200	185	120	Shear
	FC-S-W300	138	166	Shear

F_{cr} = First flexural cracking load (KN)
S_{cr} = First Shear cracking load (KN)

5.3. Load – strain reinforcement response

The load-strain curves were drawn for all the tested beams, as shown in Fig. 11. A strain gauge (S.G.) was placed on the longitudinal shear reinforcement of each beam within the expected natural load path. In the case of beams with openings, (S.G.) was placed on the compensation steel at the top of the square openings. At the beginning of applying the loads and before the occurrence of flexural cracks and shear cracks, little stress and strain occurred in the reinforcement steel, as the concrete was able to resist all the stresses applied in the initial loading stages. After that, at the beginning of the occurrence of flexural cracks and shear cracks, part of these stresses was transferred to the shear reinforcement steel, which resulted in an increase in the strains of the reinforcement steel. All the tested beams failed after the yielding of steel reinforcement.

The strain values at the ultimate load for the normal concrete beams NC-B-WO, NC-B-W200, and NC-B-W300 were 4316, 3154, and 2567 micro strain (μs), while the strain values for the fibrous beams FC-B-WO, FC-B-W200, and FC-B-W300 were 3104 , 2765, and 2335 (μs). The percentage of strain decrease was 28%, 12.34%, and 9%, respectively. It was concluded the steel fibers helped in varying proportions in reducing the stresses in the steel as they acted as a catalyst in dissipating part of these stresses. In the case of shear-bending control. It was observed that the strain values in the normal and fibrous solid beams are higher than the strain values in the beams with openings of 300 mm and 200 mm. This can be attributed to the fact that the peak load of the solid beams is much higher, and thus the stiffness is high, which leads to the values of the reinforcement steel reaching advanced stages of stress, and thus the strain values are high.

In the case of the shear control, the strain values for the normal beams NC-S-WO, NC-S-W200, and NC-S-W300 were 5188, 6010, and 7594 (μs). As for the fibrous beams, in the same order, the strain values were 4773, 5770, and 7020 (μs), where the percentages of decrease in the strain values were 8%, 4%, and 7.55%, respectively. It is also noted in the case of the shear that the solid beams have lower strains than the beams with openings of 200 mm and 300 mm. This is due to the creation of openings leading to a significant weakness in the concrete resistance, which led to the reinforcement steel in those beams bearing high and large strain values.

5.4. Ultimate load

The ultimate load values for all tested beams are summarized in Table 4. The presence of steel fibers increased the ultimate load by varying percentages between 8 and 85%. The ultimate load values for the deep beams NC-B-WO, NC-B-W200, and NC-B-W300 were 390.1 KN , 340 KN, and 127.2 KN. As for the fibrous beams of the same group, FC-B-WO, FC-B-W200, and FC-B-W300, the ultimate load values were 422.1 KN, 389.6 KN, and 236.3 KN, respectively, where the percentage of increase in the ultimate load is 8%, 14%, and 85%. It is noted that the percentage of increase in the ultimate load when steel fibers are present is large and noticeable when the size of square openings increases, which confirms the role of fibers in delaying the final failure by absorbing higher energy and significantly reducing the cracking load.

The ultimate load values for the NC-S-WO and FC-S-WO beams were 462.7 KN and 657.1 KN, where the percentage increase in the ultimate load was 42%, while for the beams with square openings of 200 mm and 300 mm, the percentage increase was 9% and 29%, respectively. Fig. 12 shows a comparison between the ultimate load for normal concrete deep beams and fibrous concrete deep beams.

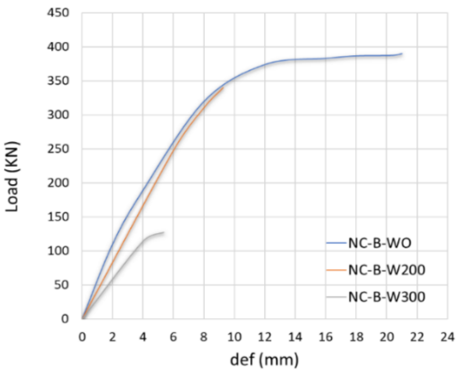

(a) Normal (Shear-bending control)

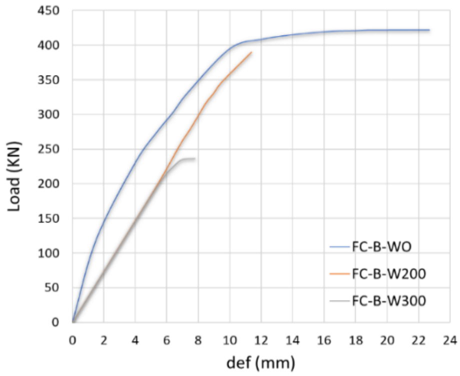

(b) Fibrous (Shear-bending control)

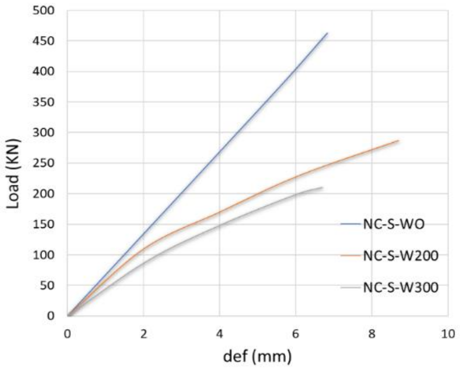

(c) Normal (shear control)

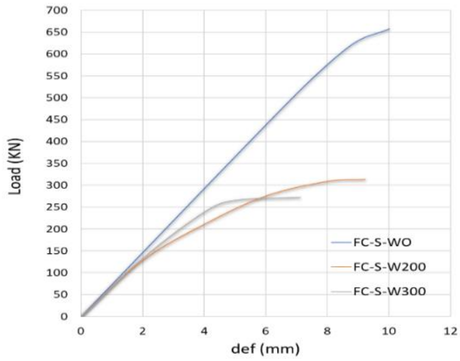

(d) Fibrous (shear control)

Fig. 10. load – deflection curve for all tested beams

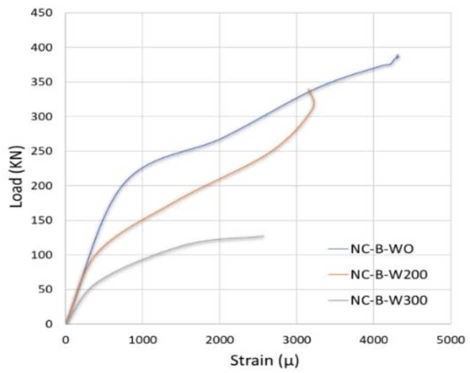

(a) Normal (Shear-bending control)

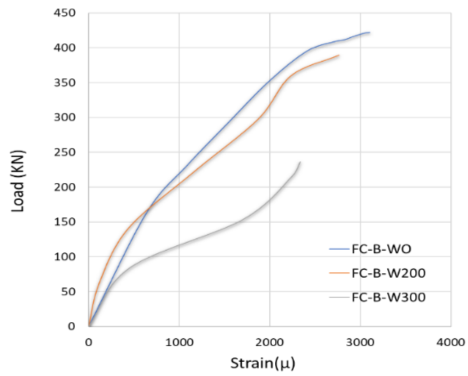

(b) Fibrous (Shear-bending control)

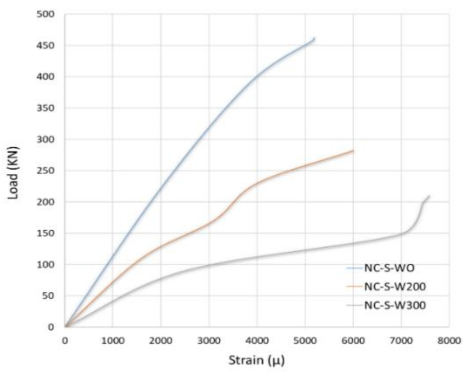

(C) Normal (shear control)

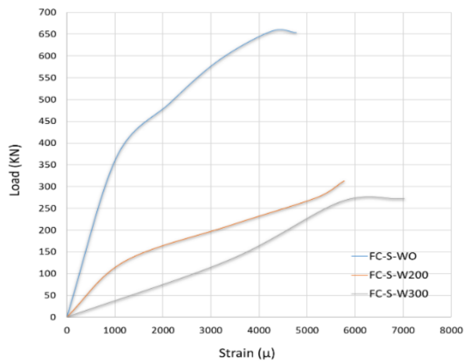

(d) Fibrous (shear control)

Fig. 11. load – strain curve for all tested beams

Table 4. Ultimate loads for all tested beams

Beam NO (Normal)	P_N	Beam NO (Fibrous)	P_F	P_F / P_N
NC-B-WO	390.1	FC-B-WO	422.1	1.08
NC-B-W200	340.0	FC-B-W200	389.6	1.14
NC-B-W300	127.2	FC-B-W300	236.3	1.85
NC-S-WO	462.7	FC-S-WO	657.1	1.42
NC-S-W200	287.0	FC-S-W200	313.0	1.09
NC-S-W300	210.0	FC-S-W300	272.0	1.29

P_N : Ultimate Load of Normal Reinforced concrete beams (KN)
P_F : Ultimate Load of Fibrous Reinforced concrete beams (KN)

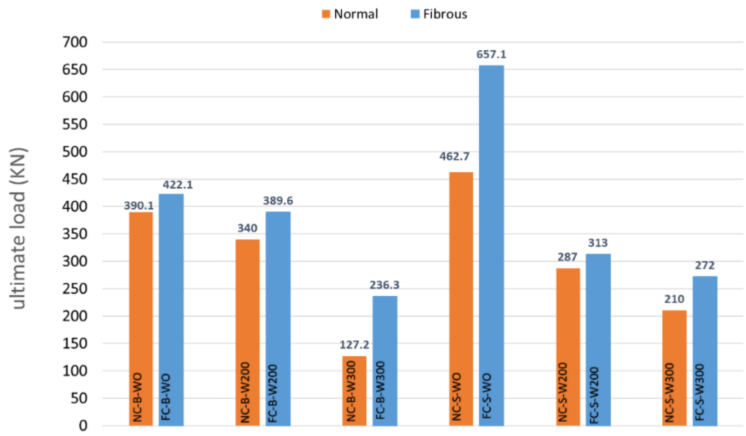

Fig. 12. Ultimate load for normal and fibrous deep beam

5.5. Effect of Web Opening

Creating openings in reinforced concrete deep beams leads to weakening the load-bearing capacity of these beams. Especially if these openings are placed in the natural load path, they lead to cracks or regions with high shear or tensile stresses. Square openings with dimensions of 200 x 200 mm and 300 x 300 mm were created in the shear span for each case of shear control and shear-bending control and compared with the solid beams, noting that the cut reinforcement for these openings was compensated at the top and bottom of these openings. Square and rectangular openings are considered worse than circular openings because the stress distribution at the edges and corners is higher and leads to high local stresses compared to circular openings.

The ultimate load values for beams FC-B-WO, FC-B-W200, and FC-B-W300 were 422.1 KN, 340 KN, and 127.2 KN, respectively. The percentages of decrease in the ultimate load of the beam with 200 mm & 300 mm openings compared to the solid beam were 8% and 44%, respectively. The ultimate load values for beams NC-S-WO, NC-S-W200, and NC-S-W300 were 390.1 KN, 340.1 KN, and 127.2 KN, respectively. The percentage decrease in the ultimate load of the beam with 200 & 300 openings was 13% and 68%, respectively. These results show the effect of increasing the size of the openings on the ultimate load through accelerating failure and the appearance of cracks and decreasing the resistance to the applied loads. Table 5 and Fig. 13 show the ratio of the ultimate load values for the beams with square openings to the solid beams.

Table 5. ratio of ultimate load for beam with opening to the solid beam

Beam NO	P_u	P_o / P_s
FC-B-WO	422.1	1.00
FC-B-W200	389.6	0.92
FC-B-W300	236.3	0.56
NC-B-WO	390.1	1.00
NC-B-W200	340.0	0.87
NC-B-W300	127.2	0.32
FC-S-WO	657.1	1.00
FC-S-W200	313.0	0.47
FC-S-W300	272.0	0.41
NC-S-WO	462.7	1.00
NC-S-W200	287.0	0.62
NC-S-W300	210.0	0.45

P_u : ultimate load for tested beams (KN)
P_o : ultimate load of beam with opening (KN)
P_s : ultimate load of solid beam (KN)

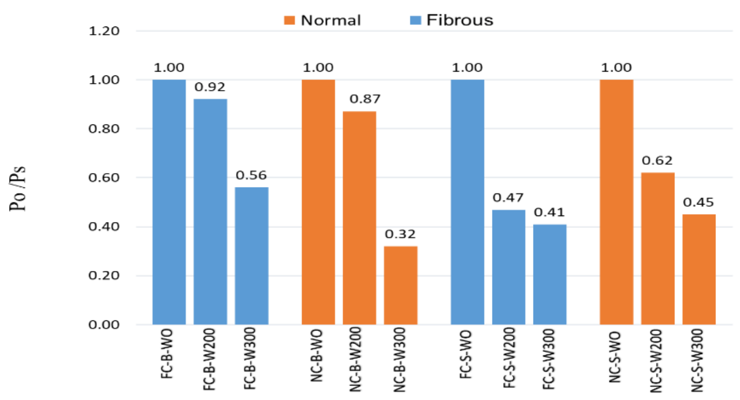

Fig. 13. Percentage decrease in ultimate load due to square openings

5.6. Stiffness

Stiffness is defined as the forces required to produce one unit of displacement. It is an important indicator of the strength and resistance of a structural member. The stiffness of a beam is influenced by several factors, including the material properties, the cross-sectional geometry, and the length of the beam.

The ACI Code 318-19 indicated that the (load-def) curve of concrete has a linear behavior in the initial loading stages , i.e., by approximately (40-50)% of the ultimate load. Therefore, and based on that, the stiffness of the tested beams was calculated by projecting 45% of the ultimate load for each beam onto the load-deflection curve to find the amount of deflection for each load on the curves. The load and deflection at that point can be considered as the yielding load and the yielding deflection. Where stiffness represents (yielding load / yielding def).

In general, except for beams NC-B-W200 and FC-B-W200, the stiffness of the fibrous concrete beams was higher than that of the normal concrete beams. The stiffness values of the NC-S-WO, NC-S-W200, and NC-S-W300 beams were 65 KN/mm, 51.66 KN/mm, and 35 KN/mm, respectively. On the other hand, for the same group, the stiffness values of the fibrous beams FC-B-WO, FC-B-W200, and FC-B-W300 were 71.95 KN/mm , 60 KN/mm, and 67 KN/mm. The increase in stiffness was 9.6%, 16.2%, and 92%. It is noted that despite the increase in the size of the openings, the increase in stiffness is at large rates when comparing the normal beams with the fibrous beams. This indicates and justifies the effect of the steel fibers. It resists cracks that are formed around the square openings between the point of applying loads and the supports.

The steel fibers contribute to resisting shear cracks by providing additional tensile strength across the cracks and bridging those cracks. Table 6 shows the stiffness values for all tested beams. The stiffness values for NC-B-WO, NC-B-W200, and NC-B-W300 were 47.43 KN/mm, 39.74 KN/mm, and 28.62 KN/mm, respectively. It is noted that for the same group, increasing the size of square openings leads to a decrease in the stiffness. Fig. 14 shows the difference between the stiffness values of normal and fibrous beams.

Ductility Index

Ductility is one of the most important properties and indicators of the behavior and resistance of the structural member. It represents the ability of the structural element to deform with the continuous application of loads after the maximum load stage, as this property works to redistribute stresses and gives sufficient warning and notice before failure occurs. In practical applications, ductility is important to ensure the ability of the structural member to withstand dynamic loads and impact loads without brittle failure. Therefore, when this ductility is high, the risk of sudden failure can be reduced by using many techniques, such as wrapping with steel or carbon fibers and others. On the contrary, when the ductility is low, this is a bad indicator of the behavior of the structural member and indicates the fragility and weakness of that member. The ductility index of all tested beams was calculated by dividing the deflection at ultimate load (Δu) by the deflection at yielding load (Δy). As shown in Table 6.

The ductility index of the fibrous concrete beams was better than that of normal concrete beams. The percentage increase in ductility varied between 1.681% and 59.27%. Fig. 15 shows the ductility values of all the tested normal and fibrous concrete deep beams. Table 7 shows the percentage increase in stiffness and ductility index of fibrous concrete deep beams compared to normal concrete deep beams.

Table 6. Stiffness and ductility index

Beam no	Pu	Δu	Py	Δy	$K\left(\frac{Py}{\Delta y}\right)$	$\mu\left(\frac{\Delta u}{\Delta y}\right)$
NC-B-WO	390.1	21.02	175.32	3.70	47.43	5.68
NC-B-W200	340.0	9.20	153.00	3.85	39.74	2.38
NC-B-W300	127.2	5.38	57.24	2.00	28.62	2.69
FC-B-WO	422.1	22.7	189.94	2.70	70.35	8.40
FC-B-W200	389.6	11.39	175.32	4.60	38.10	2.42
FC-B-W300	236.3	7.80	106.20	2.80	36.62	2.78
NC-S-WO	462.7	6.82	208.00	3.20	65.00	2.13
NC-S-W200	287.0	8.70	129.15	2.50	51.66	3.48
NC-S-W300	210.0	6.70	94.50	2.70	35.00	2.48
FC-S-WO	657.1	10.01	295.00	4.10	71.95	2.44
FC-S-W200	313.0	9.23	140.00	2.30	60.00	4.00
FC-S-W300	272.0	5.38	122.40	1.80	67.00	3.95

Pu : ultimate load (KN)
Δu : deflection at ultimate load (mm)
Py : yielding load (KN)
Δy : deflection at yielding load (mm)
K : stiffness (KN /mm)
μ : ductility index (mm /mm)

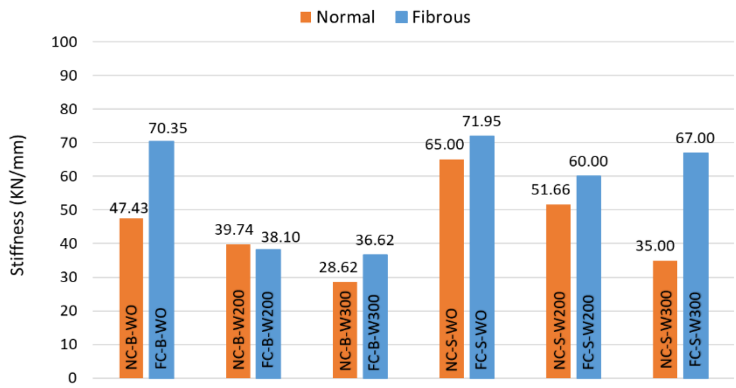

Fig. 14. Stiffness Values for Normal and Fibrous Deep beams

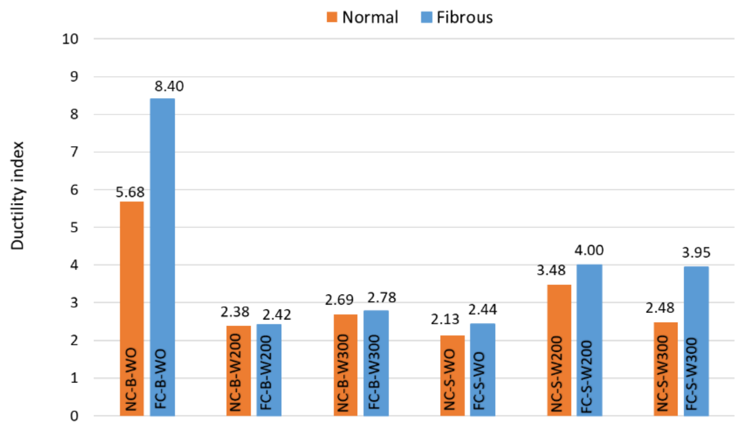

Fig. 15. Ductility index

Table 7. Increase in stiffness and ductility index

Beam NO	K_N	μ_N	Beam NO	K_F	μ_F	K_F / K_N	μ_F / μ_N
NC-B-WO	47.43	5.68	FC-B-WO	70.35	8.4	1.483	1.478
NC-B-W200	39.74	2.38	FC-B-W200	38.113	2.42	0.959	1.016
NC-B-W300	28.62	2.69	FC-B-W300	36.62	2.78	1.279	1.033
NC-S-WO	65.00	2.13	FC-S-WO	71.95	2.44	1.106	1.145
NC-S-W200	51.66	3.48	FC-S-W200	60.00	4.00	1.161	1.149
NC-S-W300	35.00	2.48	FC-S-W300	67.00	3.95	1.914	1.592

K_N : Stiffness of Normal concrete deep beam (KN /mm)
μ_N : ductility of Normal concrete deep beam (mm /mm)
K_F : Stiffness of Fibrous concrete deep beam (KN /mm)
μ_F : ductility of Fibrous concrete deep beam (mm /mm)

5.7. Energy Absorption

Creating openings in reinforced concrete deep beams leads to a reduction in their strength and capacity, which leads to a decrease in the absorption energy. The absorption energy for each tested beam can be calculated by integrating the area under the load-deflection curve. It is noted, as in Table 8 , that the absorption energy decreased significantly due to the creation of square openings in deep concrete beams. In general , the absorption energy values for all fibrous deep beams were greater than those of normal deep beams due to the role of steel fibers in increasing ductility, delaying the appearance of cracks, and providing post-cracking tensile strength. Fig.16 shows a comparison between the absorption energy of fibrous deep beams and normal deep beams.

Table 8. Absorption energy for each tested deep beam

Beam NO	E_N	Beam NO	E_F	E_F / E_N
NC-B-WO	6269.70	FC-B-WO	7719.08	1.231
NC-B-W200	1714.60	FC-B-W200	2363.00	1.378
NC-B-W300	394.34	FC-B-W300	1069.18	2.711
NC-S-WO	1567.06	FC-S-WO	3573.46	2.280
NC-S-W200	1481.25	FC-S-W200	1918.28	1.295
NC-S-W300	809.00	FC-S-W300	1323.26	1.635

E_N : Absorption energy of Normal concrete deep beam (KN.mm)
E_F : Absorption energy of Fibrous concrete deep beam (KN.mm)

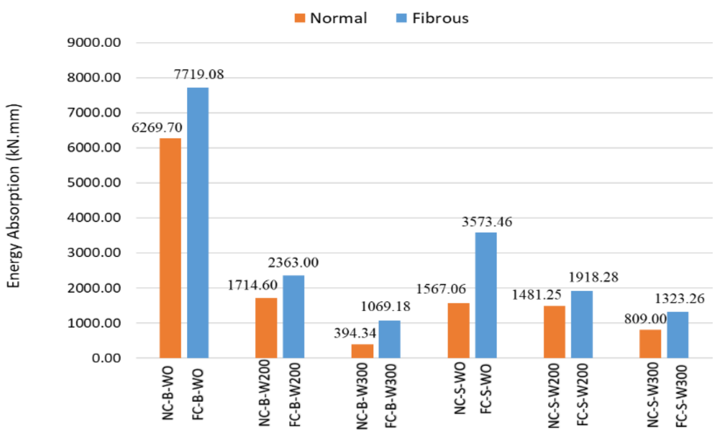

Fig. 16. Energy Absorption for normal and fibrous concrete deep beam

6. CONCLUSIONS

Based on the experimental results. The following conclusions can be drawn :

1. All the reinforced concrete deep beams tested failed as shear failure except for beams NC-B-WO and FC-B-WO, which failed as flexural failure. For the beams tested under shear-bending control, the diagonal shear cracks of the normal beams with openings NC-B-W200 and NC-B-W300 appeared before the flexural cracks. On the other hand, for fibrous beams FC-B-W200 and FC-B-W300 , the flexural cracks appeared before the diagonal shear cracks. In general, despite the introduction of square openings in the shear span of the deep beams, the addition of steel fibers delayed the appearance of diagonal shear cracks at the openings and improved the weak zone at the corners and edges around the square openings
2. In all tested beams, linear behavior is observed in the initial loading stages. It is observed in the solid beams NC-B-WO and FC-B-WO that they took on a flat character in the late loading stages and when approaching the ultimate load, indicating the high absorption energy, unlike the beams with square openings, where the creation of openings led to sudden collapse when these beams approached the ultimate load, especially since these openings were placed within the natural load path between the point of load application and the supports.
3. The steel fibers play a major role in maintaining the linear behavior until late stages of loading, and this can be clearly seen in the load-deflection curve in the deep beams containing openings. The fibrous deep beams with openings (300 x 300 mm) were almost identical until the late stages of loading with fibrous deep beams with openings (200 x 200 mm), in contrast to the beams with normal concrete, where there was a large difference in the load-deflection curves since the early stages of loading.
4. All tested beams failed after yielding of the steel reinforcement. The ultimate strain values of the reinforcement steel for the fibrous deep beams FC-B-WO, FC-B-W200, and FC-B-W300 were 8%, 4%, and 7.55% lower than the normal deep beams NC-B-WO, NC-B-W200, and NC-B-W300, respectively. It was concluded from these results that steel fibers helped in varying proportions in reducing stresses in the reinforcing steel, as steel fibers acted as a contributing factor in dissipating and absorbing part of these stresses.
5. In the case of shear-bending control, it was observed that the ultimate strain values in the normal and fibrous solid beams are higher than the strain values in the beams with openings of 300 mm and 200 mm. This can be attributed to the fact that the peak load of the solid beams is much higher, and thus the stiffness is high, which leads to the values of the reinforcement steel reaching advanced stages of stress, and thus the strain values are high. On the other side , it is also noted in the case of the shear that the solid beams have lower strains than the beams with

openings of 200 mm and 300 mm. This is due to the creation of openings leading to a significant weakness in the concrete resistance, which led to the reinforcement steel in those beams bearing large strain values

6. The ultimate load values of the fibrous beams FC-B-WO, FC-B-W200, and FC-B-W300 were higher than the ultimate load values of the normal beams NC-B-WO, NC-B-W200, and NC-B-W300 by 8%, 14%, and 85%, respectively. Also, the percentage increase in ultimate load of the fibrous beams FC-S-W200 and FC-S-W300 is 9% and 29% compared to the normal beams NC-S-W200 and NC-S-W300. It is noted that despite the increase in the size of the square openings, the steel fibers delayed the final failure, absorbed higher energy, and increased the ultimate load capacity by significant percentages.

7. The ultimate load for fibrous beams with openings FC-B-W200 and FC-B-W300 decreased to 8% and 44% compared to solid beam FC-B-WO. Also , the ultimate load for normal beams with openings NC-B-W200 and NC-B-W300 decreased to 13% and 68% compared with solid beam NC-B-WO. These results demonstrate the effect of introducing square openings on the ultimate load of deep beams, especially when they are located along the natural load path between the point of load application and the supports, as well as the concentration of stresses around corners and edges, which accelerates the appearance of diagonal shear cracks and reduces the resistance.

8. The stiffness values of the fibrous beams are higher than the normal beams. It is noted that despite the increase in the size of the openings, the increase in stiffness is at large rates when comparing normal beams with fiber beams. This indicates and justifies the effect of steel fibers, as steel fibers contribute to resisting shear cracks by providing additional tensile strength across the cracks and bridging those cracks

9. Steel fibers increase the ductility index, which is an important property as it redistributes stresses and gives sufficient warning and notice before failure occurs. The ductility values of all fiber beams were higher than the ductility values of normal beams. Also, the absorption energy values for all fibrous deep beams were greater than those of normal deep beams due to the role of steel fibers in increasing ductility, delaying the appearance of cracks, and providing post-cracking tensile strength.

7. REFERENCES

318, ACI Committee, 2019. Building Code Requirements for Structural Concrete (ACI 318-19). Farmington Hills: American Concrete Institute.

Al-Bayati, N.A., Muhammad, B.R. and Hasan, A.S., 2016. Structural Behavior of Self Compacting Reinforced Concrete Deep Beams Containing Openings. Engineering and Technology Journal, 34(12), pp.2310-2317.https://doi.org/10.30684/etj.34.12A.13

Al-Mahbashi, M., Elsanadedy, H., Abbas, H., Abadel, A. and Al-Salloum, Y., 2023. Experimental and numerical study of high strength reinforced concrete continuous deep beams with circular and rectangular openings. Journal of Building Engineering, 79, p.107868.https://doi.org/10.1016/j.jobe.2023.107868

Al-Sarraf, S.Z., Al-Shaarbaf, I.A. and Diab, A.S., 2011. Effect of steel fiber on the behavior of deep beams with and without web opening. Engineering and Technology Journal, 29(1), pp.1-19.https://doi.org/10.30684/etj.29.1.1

ASTM International, 2016. ASTM A615 / A615M-16: Standard Specification for Deformed and Plain Carbon-Steel Bars for Concrete Reinforcement. West Conshohocken, PA: ASTM International.

Attiya, M.A., 2024. Behavior of reinforced concrete continuous deep beams with openings and using multiple types of strengthening. Kufa Journal of Engineering, 15(3), pp. 1-20. https://doi.org/10.30572/2018/KJE/150301

Campione, G. and Minafò, G., 2012. Behaviour of concrete deep beams with openings and low shear span-to-depth ratio. Engineering Structures, 41, pp.294-306. https://doi.org/10.1016/j.engstruct.2012.03.055

Central Organization for Standardization and Quality Control, 2019. Iraqi Standard Specification No.5/1984. Baghdad, Iraq.

Central Organization for Standardization and Quality Control, 2019. Iraqi Standard Specification No.45/1984. Baghdad, Iraq.

El-Kareim, A., Arafa, A., Hassanin, A., Atef, M., and Saber, A., 2020, October. Behavior and strength of reinforced concrete flanged deep beams with web openings. In Structures (Vol. 27, pp. 506-524). Elsevier. https://doi.org/10.1016/j.istruc.2020.06.003

Hussain, H.K., 2018. Finite element analysis of deep beam under direct and indirect load. Kufa Journal of Engineering, 9(2), pp.152-167. http://dx.doi.org/10.30572/2018/kje/090212

Jasim, W.A., Allawi, A.A. and Oukaili, N.K., 2019. Effect of size and location of square web openings on the entire behavior of reinforced concrete deep beams. Civ. Eng. J, 5(1), pp.209-226. http://dx.doi.org/10.28991/cej-2019-03091239

Khalaf, M.R. and Al-Ahmed, A.H.A., 2021. Effect of large openings on the behavior of reinforced concrete continuous deep beams under static and repeated load. In E3S Web of Conferences (Vol. 318, p. 03012). EDP Sciences. https://doi.org/10.1051/e3sconf/202131803012

Laranjeira de Oliveira, F., 2010. Design-oriented constitutive model for steel fiber reinforced concrete. Universitat Politècnica de Catalunya. DOI 10.5821/dissertation-2117-93486

Mabrouk, R.T., Mahmoud, M.A. and Kassem, M.E., 2022. Behavior of reinforced concrete deep beams with openings under vertical loads using strut and tie model. Civil Engineering Journal, 7, pp.148-170. http://dx.doi.org/10.28991/CEJ-SP2021-07-011

Methods of testing concrete. Method for determination of compressive strength of concrete cubes (BS 1881-116:1983)

Nayak, C.B., 2022. Experimental and numerical study on reinforced concrete deep beam in shear with crimped steel fiber. Innovative Infrastructure Solutions, 7(1), p. p.41. https://doi.org/10.1007/s41062-021-00638-2

Saleh, M., Al Hamaydeh, M. and Zakaria, M., 2023. Finite element analysis of reinforced concrete deep beams with square web openings using damage plasticity model. Engineering Structures, 278, p.115496. https://doi.org/10.1016/j.engstruct.2022.115496

Shakir, Q., Yahya, Y.M. and Jasim, A., 2019. Strengthening of reinforced self-compacting concrete T-deep beam with large opening by carbon fiber sheets. Kufa Journal of Engineering, 10(2), pp.76-89. http://dx.doi.org/10.30572/2018/kje/100206

Vengatachalapathy, V. and Ilangovan, R., 2010. A study on steel fibre reinforced concrete deep beams with and without openings. International Journal of Civil & Structural Engineering, 1(3), pp.509-517.